Highly Branched Xylan Made by IRREGULAR XYLEM14 and MUCILAGE-RELATED21 Links Mucilage to Arabidopsis Seeds[1][OPEN]

Cătălin Voiniciuc*, Markus Günl, Maximilian Heinrich-Wilhelm Schmidt, and Björn Usadel

Institute for Bio- and Geosciences (IBG-2: Plant Sciences), Forschungszentrum Jülich, 52425 Jülich, Germany (C.V., M.G., M.H.-W.S., B.U.); and Institute for Botany and Molecular Genetics, BioEconomy Science Center, RWTH Aachen University, 52074 Aachen, Germany (C.V., M.H.-W.S, B.U.)

ORCID IDs: 0000-0001-9105-014X (C.V.); 0000-0003-4576-6774 (M.H.-W.S.).

All cells of terrestrial plants are fortified by walls composed of crystalline cellulose microfibrils and a variety of matrix polymers. Xylans are the second most abundant type of polysaccharides on Earth. Previous studies of Arabidopsis (*Arabidopsis thaliana*) *irregular xylem* (*irx*) mutants, with collapsed xylem vessels and dwarfed stature, highlighted the importance of this cell wall component and revealed multiple players required for its synthesis. Nevertheless, xylan elongation and substitution are complex processes that remain poorly understood. Recently, seed coat epidermal cells were shown to provide an excellent system for deciphering hemicellulose production. Using a coexpression and sequence-based strategy, we predicted several *MUCILAGE-RELATED* (*MUCI*) genes that encode glycosyltransferases (GTs) involved in the production of xylan. We now show that MUCI21, a member of an uncharacterized clade of the GT61 family, and IRX14 (GT43 protein) are essential for the synthesis of highly branched xylan in seed coat epidermal cells. Our results reveal that xylan is the most abundant xylose-rich component in Arabidopsis seed mucilage and is required to maintain its architecture. Characterization of *muci21* and *irx14* single and double mutants indicates that MUCI21 is a Golgi-localized protein that likely facilitates the addition of xylose residues directly to the xylan backbone. These unique branches seem to be necessary for pectin attachment to the seed surface, while the xylan backbone maintains cellulose distribution. Evaluation of *muci21* and *irx14* alongside mutants that disrupt other wall components suggests that mucilage adherence is maintained by complex interactions between several polymers: cellulose, xylans, pectins, and glycoproteins.

All cells of terrestrial plants are fortified by walls composed of polysaccharides, proteins, and phenolic compounds. Composites of crystalline cellulose microfibrils and a variety of matrix polymers form strong yet resilient extracellular structures (Cosgrove, 2005). Cellulose is the main load-bearing component of plant cell walls and consists of linear β-1,4-linked Glc chains, which are synthesized and assembled into microfibrils at the plasma membrane. Most other wall polysaccharides have more complex structures, can be branched, and are usually synthesized in the Golgi apparatus by coordinated action of glycosyltransferase (GT) enzymes (Oikawa et al., 2013). While pectic polymers (homogalacturonan [HG], rhamnogalacturonan [RG], and xylogalacturonan [XGA]) are rich in uronic acids, hemicelluloses (xylans, xyloglucans [XyGs], and heteromannans) have backbones of neutral sugars that can interact with cellulose via hydrogen bonds (Somerville et al., 2004). Xylans are the second most abundant class of polysaccharides on Earth, but they cannot be efficiently utilized for biofuels because they consist predominantly of pentose sugars, which are difficult to ferment by microorganisms such as yeast (*Saccharomyces cerevisiae*; Rennie and Scheller, 2014). Xylans from cereal-derived foods are important for human nutrition but are largely indigestible without the complex and dynamic polysaccharide-degrading machinery of the gut microbiota (Rogowski et al., 2015). The xylan backbone consists of β-1,4-linked Xyl residues and is substituted with acetyl groups and different carbohydrates, typically GlcA in dicots and Ara in monocots (Faik et al., 2014). Even within one species, xylan structure can differ between the primary walls and the secondary walls, which are deposited after cell

[1] This work was supported by the Natural Sciences and Engineering Research Council of Canada (PGS-D3 grant to C.V.), the Ministry of Innovation, Science, and Research of North-Rhine Westphalia within the framework of the North-Rhine Westphalia Strategieprojekt BioEconomy Science Center (grant no. 313/323–400–00213 to M.H.-W.S. and B.U.). Generation of the antibodies and substrates was supported by the National Science Foundation Plant Genome Program (grant no. DBI–0421683), and generation of the UDP-Xylose was supported in part by the Complex Carbohydrate Research Center (grant no. DE–FG02–93ER20097).

* Address correspondence to c.voiniciuc@fz-juelich.de.

The author responsible for distribution of materials integral to the findings presented in this article in accordance with the policy described in the Instructions for Authors (www.plantphysiol.org) is: Cătălin Voiniciuc (c.voiniciuc@fz-juelich.de).

C.V. designed the research and wrote the article, with valuable advice from M.G. and B.U.; M.H.-W.S. performed the cloning and *Escherichia coli* work; M.G. performed the monosaccharide and glycosyl linkage analyses; C.V. performed the remaining experiments; C.V., M.G., M.H.-W.S., and B.U. read and approved the final article.

[OPEN] Articles can be viewed without a subscription.

www.plantphysiol.org/cgi/doi/10.1104/pp.15.01441

expansion is completed (Mortimer et al., 2015). Xylans play important roles in strengthening secondary walls because most xylan-deficient mutants have collapsed xylem vessels, dwarfed stature, and reduced fertility (Scheller and Ulvskov, 2010). Analysis of Arabidopsis (*Arabidopsis thaliana*) *irregular xylem* (*irx*) mutants enabled the discovery of many genes required for xylan biosynthesis (Brown et al., 2007; Faik et al., 2014).

Even though the xylan backbone is a homopolymer, multiple Golgi-localized putative xylosyltransferases (XylTs) from two different protein families are required for its elongation (Rennie and Scheller, 2014). IRX10 (a GT47 enzyme) and IRX9 and IRX14 (two GT43 members) are involved in xylan synthesis together with their functionally redundant paralogs, IRX10-LIKE (IRX10-L), IRX9-L, and IRX14-L. These three sets of genes play distinct roles in xylan synthesis, and double mutants lacking any of the pairs have either little to no xylan compared with the wild type (Brown et al., 2009; Lee et al., 2010; Wu et al., 2010). So far, only IRX10 and IRX10-L proteins were unambiguously demonstrated to function as xylan synthases in vitro (Jensen et al., 2014; Urbanowicz et al., 2014). Although *IRX9* and *IRX14* expression promotes xylan XylT activity in Arabidopsis and tobacco (*Nicotiana tabacum*) microsomes (Lee et al., 2010, 2012b; Wu et al., 2010), their biochemical functions are unclear. Based on site-directed mutagenesis experiments, IRX9 and IRX14 are unlikely to be catalytically active, because they can function without the conserved amino acids required for mammalian GT43 enzymes (Ren et al., 2014). These proteins might therefore play structural roles in a xylan synthase complex with IRX10/IRX10-L at its core. IRX14 could potentially bind UDP-Xyl (the donor substrate for xylan synthesis) via its DxD motif and pass it to the IRX10 enzyme (Ren et al., 2014).

The diversity of xylan side chains, which vary in a species- and tissue-specific manner, adds another layer of complexity to the complicated biosynthetic mechanism described above. In Arabidopsis, the GlcA substitution of xylan (GUX) is catalyzed by a group of enzymes from the GT8 family (Lee et al., 2012a; Rennie et al., 2012). Because GUX1 and GUX2 decorate distinct xylan domains in Arabidopsis secondary walls, *gux1 gux2* double mutant stems have largely unbranched xylans (Mortimer et al., 2010; Bromley et al., 2013). Surprisingly, these mutants have normal xylan backbone content, demonstrating that the elongation and substitution of xylan can be uncoupled in Arabidopsis (Mortimer et al., 2010). By contrast, evidence from grass suggests that xylan elongation and substitution are coupled (Faik et al., 2014). The addition of arabinoxylan side chains in monocots requires at least two distinct groups of proteins from the GT61 family (Anders et al., 2012; Chiniquy et al., 2012). Although there are several putative homologs in the Arabidopsis genome, their functions remain to be investigated.

While Ara-decorated xylan has not been reported in Arabidopsis secondary walls, the seed mucilage of another dicot, psyllium (*Plantago ovata*), is rich in arabinoxylan and was successfully exploited to discover genes involved in the production of this polysaccharide (Jensen et al., 2011, 2013, 2014). Mucilage is a specialized wall, containing hydrophilic polysaccharides, that swells upon hydration and can play important roles in promoting seed dispersal and germination (Western, 2011). Transcriptional profiling indicates that only IRX10 (without IRX9 and IRX14) might be required to synthesize the xylan backbone in psyllium mucilage and that multiple GT61 proteins may be responsible for the various xylan substitutions in this specialized wall (Jensen et al., 2013). Although Arabidopsis seed mucilage primarily consists of the pectic polymer RG I, glycosyl linkage analysis suggests that highly branched xylans are also present (Naran et al., 2008; Walker et al., 2011; Voiniciuc et al., 2015b).

The Arabidopsis seed coat epidermal (SCE) cells represent a great model to study the synthesis and secretion of polysaccharides (for review, see Haughn and Western, 2012; North et al., 2014; Voiniciuc et al., 2015b). Although more than 35 genes are known to affect the structure of mucilage (Voiniciuc et al., 2015b), most of the GTs necessary for the synthesis of its components remain unknown. The architecture of distinct polymers in mucilage influences three major properties of this hydrogel: (1) release from SCE cells, (2) attachment to the seed, and (3) mucilage density or compactness. The release of mucilage upon hydration depends on correct branching of RG I and on HG methylesterification (Dean et al., 2007; Macquet et al., 2007; Rautengarten et al., 2008; Arsovski et al., 2009; Saez-Aguayo et al., 2013; Voiniciuc et al., 2013). An adherent capsule, representing 35% of the total mucilage produced (Voiniciuc et al., 2015b), is anchored around each seed and is associated with ray-like structures synthesized in part by CELLULOSE SYNTHASE (CESA) proteins (Harpaz-Saad et al., 2011; Mendu et al., 2011; Sullivan et al., 2011; Griffiths et al., 2015) and potentially assembled by COBRA-LIKE2 (Ben-Tov et al., 2015). Two additional proteins, SALT-OVERLY SENSITIVE5 (SOS5; also annotated as FASCICLIN-LIKE ARABINOGALACTAN PROTEIN4 [FLA4]) and the receptor-like kinase FEI2 (named after the Chinese word for fat) are required for mucilage adherence, but their functions remain unclear (Harpaz-Saad et al., 2011; Griffiths et al., 2014). Arabinogalactan proteins can be covalently linked to both RG I and arabinoxylan (Tan et al., 2013), so SOS5/FLA4 could potentially link two structures (Griffiths et al., 2014).

Recently, heteromannan produced by CELLULOSE SYNTHASE-LIKE A2 (Yu et al., 2014) and MUCILAGE-RELATED10 (MUCI10; Voiniciuc et al., 2015a) was shown to control the density of polysaccharides in the mucilage capsule. Using a coexpression and sequence-based strategy, we predicted that *MUCI10* (GT34 member) is a mucilage biosynthetic gene. Our in-depth biochemical and physiological characterization of *MUCI10* shows that this reverse genetic approach is successful to discover GTs required for cell wall polysaccharide production (Voiniciuc et al., 2015a). By

extending this screen, we identified At3g10320 (*MUCI21*), which belongs to an uncharacterized GT61 clade and three genes involved in xylan elongation (*IRX9*, *IRX10*, and *IRX14*) as promising candidates for mucilage synthesis. We demonstrate that highly branched xylan made by IRX14 and MUCI21 is the main Xyl-rich polymer in mucilage. XyG and XGA are absent from mucilage or are not essential for its properties. We also show that Arabidopsis SCE cells produce a unique xylan structure, whose branches are seem to be necessary for pectin attachment to the seed surface and whose backbone mediates cellulose architecture. Comparison of *muci21* and *irx14* mucilage defects to those of *cesa5*, *fei2*, or *sos5* mutants suggests that adherence is maintained by complex interactions between several wall polymers.

RESULTS

MUCI21 Is Required for the Synthesis of Xyl-Rich Mucilage Polymers

At3g10320 (annotated as *MUCI21*) is a promising candidate from the *MUCI* screen, as it was coexpressed with known mucilage genes in the GeneCAT and GeneMANIA tools (Mutwil et al., 2008; Warde-Farley et al., 2010) and had the hallmarks of a GT protein. MUCI21 is related to enzymes from the GT61 family and belongs to the hitherto uncharacterized clade B (Fig. 1). We identified two to five clade B proteins in each of the plants selected for our phylogenetic analysis: *Physcomitrella patens*, *Selaginella moellendorffii*, rice (*Oryza sativa*) 'japonica,' *Populus trichocarpa*, and Arabidopsis. In contrast to this group of unknown proteins, a few members of clades A and C have already been characterized. The distantly related Arabidopsis XYLT enzyme (GT61 clade C; Fig. 1) catalyzes the β-1,2-xylosylation of *N*-glycans (Strasser et al., 2000; Kajiura et al., 2012). Our phylogenetic analysis indicates that plants typically have only one clade C isoform (Fig. 1), while clade A has 8-fold more members in rice than Arabidopsis and is likely involved in the arabinoxylan substitution. Xylan α-1,3-arabinosyltransferase (XAT) and xylan β-1,2-XylT (XAX) enzymes add xylan side chains that typically distinguish grasses from dicots (Anders et al., 2012; Chiniquy et al., 2012).

Microarray analysis of developing Arabidopsis seeds shows that *MUCI21* is specifically expressed in the seed coat at the linear cotyledon and mature green stages, when mucilage synthesis occurs (Fig. 2A; Winter et al., 2007; Belmonte et al., 2013). Using quantitative reverse transcription (qRT)-PCR and *UBIQUITIN5* (*UBQ5*) as a

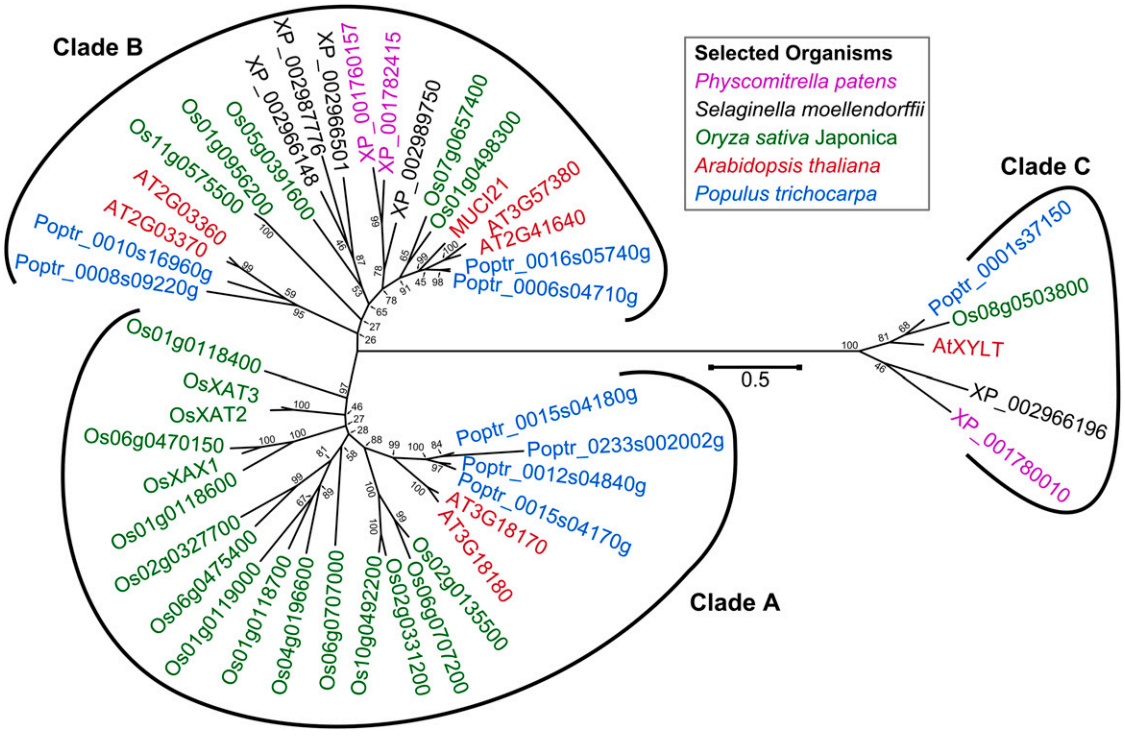

Figure 1. Phylogenetic tree of GT61 proteins from five species. Branches are annotated with National Center for Biotechnology Information Reference sequences, except for the known AtXYLT, OsXAT2, OsXAT3, and OsXAX1 enzymes. Clades are named as first reported (Anders et al., 2012). MUCI21 belongs to the hitherto uncharacterized clade B of the GT61 family. The tree is drawn to scale, with branch lengths measured in the number of substitutions per site. Bootstrap values indicate the reliability of the nodes.

reference gene, we confirmed the elevated expression of *MUCI21* in developing siliques at the linear and mature green stages (Fig. 2C). Two independent insertions in *MUCI21* (Fig. 2B) did not dramatically alter expression at the 5′ end (before the mutations) but knocked out more than 90% of transcription at the 3′ end (Fig. 2D), which encodes the Domain of Unknown Function (DUF)563 conserved in all GT61 proteins. Therefore, the partial transcripts detected in *muci21* homozygous mutants are unlikely to encode functional peptides. Both alleles showed equally severe defects in seed mucilage staining with ruthenium red (RR), a pectin dye (Fig. 3, A–C). Adherent mucilage capsules were dramatically reduced for *muci21-1* and *muci21-2* compared with the wild type, whereas the total amounts of mucilage sugars were not significantly altered (Fig. 3I). Interestingly, the Xyl content was reduced by about 60% in the two *muci21* alleles (Fig. 3J; Table I), despite normal amounts of all other monosaccharides (Table I). This suggests that MUCI21 is involved in the synthesis of Xyl-rich polysaccharides in seed mucilage.

IRX14 and MUCI21 Are Essential For Xylan Synthesis in SCE Cells

Xylan is likely a component of mucilage, although the identity of Xyl-rich polymers in this specialized cell wall was not previously confirmed (Voiniciuc et al., 2015b). Interestingly, our reverse genetic search for *MUCI* genes yielded three players that facilitate xylan backbone elongation in Arabidopsis stems: *IRX14* (*MUCI64*), *IRX9* (*MUCI65*), and *IRX10* (*MUCI69*). These three genes resembled the expression profile of *MUCI21* during seed development (Fig. 2A; Supplemental Fig. S1), while their respective paralogs were broadly expressed (Winter et al., 2007; Belmonte et al., 2013). Another microarray analysis of dissected seed coats indicates that *MUCI21*, *IRX9*, *IRX10*, and *IRX14* are abundant at 7 d post anthesis, the peak of mucilage biosynthesis, in both the wild type and the *apetala2* (*ap2*) mutant (Supplemental Fig. S2B; Dean et al., 2011). Because *ap2* fails to develop mucilage secretory cells (Dean et al., 2011), these results suggest that the genes are not expressed only in SCE cells, although differences between the genotypes could be masked by the high standard deviations of many samples (Supplemental Figure S2B, asterisks). Even though the two available seed coat microarray data sets did not strongly agree in this instance (Dean et al., 2011; Belmonte et al., 2013), the predicted *MUCI* genes represented good candidates for mucilage biosynthesis.

Therefore, we examined the mucilage phenotypes of *irx9*, *irx10* (Supplemental Table S1), and *irx14* (Fig. 2B) homozygous mutants. Although *irx9* plants displayed severe dwarfism and were largely infertile (Brown et al., 2005), only insertions in *IRX14* disrupted seed mucilage properties (Fig. 3; Supplemental Fig. S3). Consistent with the seed expression profiles (Fig. 2A), qRT-PCR analysis showed that *IRX14* and *MUCI21* were highly expressed in siliques at the linear cotyledon and mature green stages (Fig. 2C), when secondary wall synthesis occurs. The *irx14-1* (Brown et al., 2007) and *irx14-2* (Fig. 2D) knockout mutants produced wild-type amounts of total mucilage (Fig. 3I) but lacked approximately 90% of the Xyl residues (Fig. 3J; Table I). Because IRX14 is essential for the synthesis of the xylan backbone (Brown et al., 2007; Lee et al., 2010; Wu et al., 2010; Mortimer et al., 2015), the severe Xyl deficiency of *irx14* mucilage indicates that xylan is the primary source of this monosaccharide. Both *irx14-1* and *irx14-2*, as well as a third independent allele (*irx14-3*), displayed a complete loss of adherent mucilage (Fig. 3, E–G), suggesting that xylan may be required for the attachment

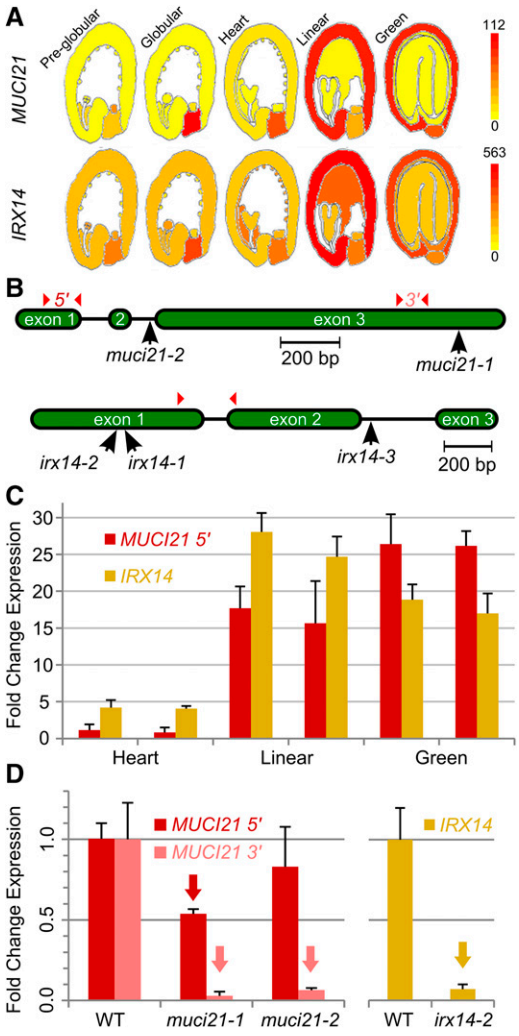

Figure 2. Overview of *MUCI21* and *IRX14* expression and mutations. A, *MUCI21* and *IRX14* are expressed in the seed coat (Winter et al., 2007; Belmonte et al., 2013). B, Insertions and qRT-PCR primers (arrowheads) used. C, Transcription in wild-type (WT) siliques stages based on embryo shape (two biological replicates each). All values are relative to the first *MUCI21* sample. D, Mutant siliques at the linear stage have reduced expression (arrows; Student's *t* test, $P < 0.05$) relative to the wild type. Data in C and D show the means + SD (normalized to *UBQ5*) of three technical replicates.

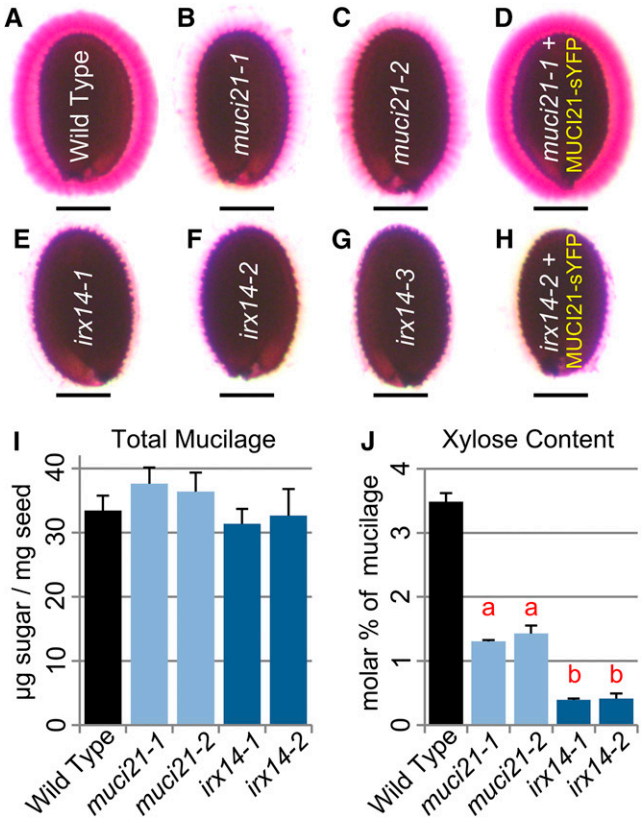

Figure 3. *muci21* and *irx14* mutants have seed mucilage defects. A to H, Seeds hydrated in water were stained with RR. The *35S:MUCI21-sYFP* transgene rescued *muci21-1* staining defects (D) but not the *irx14-2* phenotype (H). The *muci21* and *irx14* mutants produced normal amounts of total mucilage (I) but had severe decreases in Xyl content (J). Letters in J indicate significant changes between the mutants and wild type (WT; Student's *t* test, $P < 10^{-5}$). Bars = 200 μm.

of mucilage to the seed. Because similar mucilage properties were disrupted in *muci21* mutants (Fig. 3), albeit to lesser extent, we speculated that MUCI21 might also be involved in xylan biosynthesis. The reduced levels of Xyl in *irx14* and *muci21* homozygous mutants (Fig. 3J; Table I) were heritable in the offspring (Supplemental Table S2).

To investigate if, in addition to xylan, mucilage contains other Xyl-containing polymers that are important for its architecture, we analyzed the mucilage phenotypes of mutants that disrupt XyG and XGA synthesis. Although five *XyG XylT* (*XXT*) genes and *XGA DEFICIENT1* (*XGD1*) are expressed in seeds, they are not tightly associated with mucilage production in SCE cells (Supplemental Fig. S2, A and C; Winter et al., 2007; Dean et al., 2011; Belmonte et al., 2013). The *XXT* genes and *XGD1*, unlike *MUCI21* and *IRX14*, did not satisfy the requirements of our coexpression strategy and do not represent *MUCI* candidate genes. Accordingly, knockout mutations in these genes (Supplemental Table S1) did not alter the RR staining, total mucilage amounts, or the relative Xyl content (Supplemental Fig. S3). Even the *xxt1;2;5* triple mutant, which lacks detectable XyG in other Arabidopsis tissues (Zabotina et al., 2012), had normal mucilage structure (Supplemental Fig. S3). In contrast to xylan polymers, XyG and XGA are therefore absent from mucilage or are not essential for its properties.

Unlike typical dicot secondary cell walls, mucilage does not contain glucuronoxylan, as we detected only trace levels of GlcA (approximately 0.05 mol %), and *gux* mutants displayed normal mucilage properties (Supplemental Fig. S3, D and E). While *irx14-2* had 50% less Xyl and GlcA in stem cell walls, *muci21-1* and *muci21-2* mutants did not exhibit reductions in glucuronoxylan content or any other changes in stem monosaccharide composition (Supplemental Fig. S4). These data suggest that MUCI21 is specifically involved in the synthesis of unusual xylan polysaccharides in Arabidopsis seed mucilage.

Arabidopsis Seed Mucilage Contains a Unique, Highly Branched Xylan

Glycosyl linkage analysis of *muci21-1* and *irx14-2* total mucilage extracts (Table II) revealed specific changes in the abundance and structure of xylan (Table III). Relative to the wild type, only terminal-Xyl (t-Xyl) and branched 2,4-Xyl linkages were reduced by up to 90% in two independent analyses of *muci21-1*, whereas the unbranched 4-Xyl linkage was not significantly altered (Fig. 4A; Table II; Supplemental Table S3). The *muci21-1* mutant had a low degree of xylan branching (7%–10%) compared with the wild type (28%–45%; Table II; Supplemental Table S3). By contrast, *irx14-2* mucilage had 95% less unbranched 4-Xyl than the wild type and no detectable 2,4-Xyl units (Fig. 4A), consistent with a nearly complete loss of xylan. Mucilage does not seem to contain arabinoxylan, similar to other Arabidopsis secondary walls (Rennie and Scheller, 2014), because *muci21-1* and *irx14-2* had no significant changes in Ara linkages (Table II; Supplemental Table S3). Therefore, the xylan backbone in Arabidopsis mucilage is most likely decorated with single t-Xyl linkages rather than typical GlcA or Ara residues. Because related proteins from clades A and C of the GT61 family were reported to function as β-1,2-XylTs (Fig. 1; Strasser et al., 2000; Chiniquy et al., 2012), we hypothesized that MUCI21 may facilitate the addition of β-1,2-Xyl units directly to the xylan backbone (Fig. 4C).

To corroborate the glycosyl linkage data, we then quantified the amount of unbranched xylan in total mucilage extracts using the LM10 monoclonal antibody (McCartney et al., 2005), which cannot label wild-type Arabidopsis seed mucilage in situ (Young et al., 2008). As expected, enzyme-linked immunosorbent assays (ELISAs) did not detect LM10 epitopes above background levels in both the wild type, which contains highly branched xylan (Fig. 4A; Voiniciuc et al., 2015b), and in the *irx14-2* mucilage (Fig. 4B), which is almost devoid of xylan. However, unbranched xylan labeled

Table I. *Monosaccharide composition of total mucilage extracts*

Relative monosaccharide composition (mol %) and total mucilage content (micrograms of sugar per milligram of seed). Values represent the mean ± SD of four (wild type and *irx14-2*) or three (other genotypes) biological replicates.

Sugar	Wild Type	*muci21-1*	*muci21-2*	*irx14-1*	*irx14-2*
Rha	41.39 ± 1.72	45.18 ± 0.27	44.07 ± 0.15	38.96 ± 0.49	43.51 ± 1.59
Ara	1.23 ± 0.20	1.08 ± 0.03	1.07 ± 0.16	1.24 ± 0.06	1.14 ± 0.10
Gal	3.50 ± 0.32	2.50 ± 0.16	2.89 ± 0.13	3.30 ± 0.34	3.24 ± 0.51
Glc	0.72 ± 0.04	0.59 ± 0.04	0.69 ± 0.01	0.70 ± 0.03	0.73 ± 0.12
Xyl	3.48 ± 0.13	1.30 ± 0.02[a]	1.43 ± 0.12[a]	0.40 ± 0.02[a]	0.42 ± 0.08[a]
Man	0.58 ± 0.02	0.50 ± 0.02	0.61 ± 0.01	0.65 ± 0.02	0.63 ± 0.07
GalA	49.09 ± 1.16	48.85 ± 0.28	49.24 ± 0.16	54.75 ± 0.61	50.34 ± 2.21
Total	33.44 ± 2.29	37.63 ± 2.49	36.38 ± 2.96	31.34 ± 2.34	32.67 ± 4.13

[a]Significant difference (Student's *t* test, $P < 10^{-5}$) from the wild type.

by the LM10 antibody was abundant in *muci21-1* mucilage (Fig. 4B), confirming the results of the linkage analysis (Fig. 4A). Therefore, MUCI21 appears to be responsible for the high branching degree of xylan polysaccharides in this specialized wall.

MUCI21 Decorates Xylan Produced by IRX14 in Seed Mucilage

Wild-type mucilage likely contains a unique xylan structure, whose backbone is produced by IRX14 and is frequently decorated with single Xyl units by MUCI21 (Fig. 4C). We isolated a *muci21-1 irx14-2* double mutant and found that it was biochemically indistinguishable from the *irx14-2* single mutant (Fig. 3K), consistent with our model (Fig. 4C). Moreover, we expressed MUCI21 proteins tagged with yellow super fluorescent protein (sYFP) under the control of the *35S* promoter. The *35S*:*MUCI21-sYFP* transgene fully complemented the *muci21-1* staining defects (Fig. 3D) but did not even partially rescue the *irx14-2* mucilage phenotype (Fig. 3K). The MUCI21-sYFP fusion proteins restored the *muci21-1* Xyl content to wild-type levels (Fig. 4D) and were localized in small intracellular punctae, unlike the sYFP alone or the negative control (Fig. 5, A–C). In addition, the punctae of both MUCI21-sYFP (Fig. 5D) and Wave22Y (Fig. 5F), a Golgi marker (Geldner et al., 2009), aggregated in large compartments after a 60-min treatment with 100 μg mL^{-1} Brefeldin A (BFA), an inhibitor of the secretory system (Nebenführ et al., 2002). Colocalization with the Golgi marker sialyltransferase (ST)-red fluorescent protein (RFP) (Fig. 5, H–J) showed that MUCI21-sYFP proteins were present at the site of xylan biosynthesis (Fig. 4C). Although MUCI21 likely functions as a XylT required for xylan substitution in vivo, we could not confirm its enzymatic activity in vitro. Relative to controls, glutathione *S*-transferase (GST) tagged MUCI21 soluble proteins purified from *Escherichia coli* were not able to add Xyl units from UDP-Xyl to xylan oligosaccharides with several degrees of polymerization (2–6), cellohexaose, or RG I (Supplemental Fig. S5). Similarly, *Nicotiana benthamiana* microsomes expressing full-length MUCI21 proteins tagged with YFP did not incorporate [^{14}C]Xyl into xylohexaose (B. Ebert and H. Scheller, personal communication).

Highly Branched Xylan Is Required for Mucilage Adherence to Seeds

Despite producing total mucilage amounts similar to the wild type, *muci2*, and *irx14* seeds were surrounded by very small or no RR-stained capsules, respectively (Fig. 3) after 5 min of gentle shaking. To investigate this discrepancy, we hydrated seeds directly in RR and imaged them without any shaking. Consistent with the biochemical data, both *muci21* and *irx14* mutants released copious amounts of mucilage (Fig. 6, A–F). However, unlike the wild type, most of the mucilage immediately detached from the *muci21* and *irx14* seeds and dispersed into the surrounding solution. These mucilage detachment defects could not be rescued by the addition or removal of Ca^{2+} ions (Supplemental Fig. S6). Within a minute of hydration, wild-type seeds sank to the bottom of tubes containing water (Fig. 6G), because they were covered by dense hydrogels (Fig. 3A). Due to the loss of mucilage attachment (Figs. 3 and 6, A–F), most *irx14* seeds and some *muci21* seeds floated even after prolonged contact with water (Fig. 6, H–L). The *irx14* seeds floated for several days and germinated at the water surface (data not shown).

We then compared *muci21* and *irx14* to three other mutants that display impaired mucilage attachment (Fig. 7). Insertions in *MUCI21*, *IRX14*, *CESA5*, *FEI2*, or *SOS5* reduced the average size of mucilage capsules compared with the wild type, without decreasing seed size (Fig. 7A). The adherent mucilage layers of *muci21*, *irx14*, *cesa5*, and *fei2* mutants were 64% to 79% smaller than the wild type, while *sos5* had 46% smaller mucilage capsules but 14% larger seeds (Student's *t* test, $P < 10^{-3}$). More than 90% of total RG I sugars from all five mutants were extracted by gentle shaking, in contrast to wild-type mucilage where only 72% of RG I sugars did not adhere to the seed (Fig. 7B). Consistent with its

Table II. *Glycosyl linkages in total mucilage extracts*

Mean relative abundance (mol %) of each linkage ± SD of three or two (*irx14-2*) biological replicates.

Linkage	Wild Type	*muci21-1*	*irx14-2*
Rha			
t-Rha	1.68 ± 1.38	1.12 ± 0.24	3.74 ± 2.38
2-Rha	31.89 ± 0.54	26.37 ± 4.14	30.62 ± 0.17
2,3-Rha	1.40 ± 0.57	2.76 ± 1.25	1.46 ± 0.10
2,4-Rha	0.96 ± 0.71	3.35 ± 1.78	0.99 ± 0.66
Ara			
t-Ara	0.15 ± 0.08	0.05 ± 0.03	0.13 ± 0.00
5-Ara	0.09 ± 0.01	0.46 ± 0.03[a]	0.15 ± 0.10
3-Ara	0.62 ± 0.09	0.40 ± 0.04[a]	0.62 ± 0.15
Gal			
t-Gal	0.42 ± 0.17	0.28 ± 0.05	0.22 ± 0.06
2-Gal	0.17 ± 0.01	0.13 ± 0.02[a]	0.13 ± 0.08
4-Gal	0.20 ± 0.04	0.15 ± 0.02	0.12 ± 0.00
6-Gal	0.09 ± 0.01	0.10 ± 0.03	0.18 ± 0.03[a]
2,4-Gal	0.11 ± 0.09	0.12 ± 0.01	0.09 ± 0.02
4,6-Gal	0.18 ± 0.04	0.13 ± 0.02	0.18 ± 0.17
3,6-Gal	0.43 ± 0.15	0.48 ± 0.03	0.39 ± 0.18
Glc			
t-Glc	0.03 ± 0.00	0.09 ± 0.01[a]	0.03 ± 0.00
4-Glc	0.79 ± 0.03	0.71 ± 0.11	0.69 ± 0.11
3,4-Glc	0.03 ± 0.01	0.03 ± 0.01	0.05 ± 0.00
4,6-Glc	0.09 ± 0.02	0.13 ± 0.01	0.14 ± 0.05
Xyl			
t-Xyl	0.52 ± 0.08	0.15 ± 0.0[a]	0.25 ± 0.03[a]
4-Xyl	1.83 ± 0.02	1.18 ± 0.10[a]	0.10 ± 0.04[a]
2,4-Xyl	0.73 ± 0.19	0.09 ± 0.02[a]	0.00 ± 0.00[a]
Man			
4-Man	0.24 ± 0.02	0.23 ± 0.06	0.22 ± 0.11
4,6-Man	0.56 ± 0.03	0.54 ± 0.08	0.46 ± 0.02[a]
GalA			
t-GalA	0.63 ± 0.24	0.40 ± 0.08	0.71 ± 0.47
4-GalA	54.22 ± 1.60	54.31 ± 2.15	56.37 ± 1.23
2,4-GalA	0.54 ± 0.14	1.07 ± 0.34	0.51 ± 0.06
4,6-GalA	1.32 ± 0.87	5.09 ± 2.81	1.36 ± 1.18

[a]Significant difference (Student's *t* test, $P < 0.05$) from the wild type.

severe staining defects (Fig. 3), *irx14* mucilage was easier to detach relative to the other mutants, and more than 96% of its RG I sugars did not adhere to the seed (Fig. 7B). Because *cesa5*, *fei2*, and *sos5* did not have decreased Xyl content (data not shown), adherence of mucilage to the seed is likely maintained by several polymers.

Highly Branched Xylan Attaches Mucilage Pectin to Cellulosic Rays

To further investigate which components are required for the adherence of mucilage to the seed, we examined the in situ distribution of different polysaccharides. When stained with the Pontamine Fast Scarlet 4B (S4B) dye, *muci21* seeds showed cellulosic rays that were more similar to the wild type than to *cesa5*, *sos5*, or *muci10* mutants (Fig. 8). While *muci21* did not show any dramatic cellulose defects, a nearly total loss of xylan in *irx14* resulted in irregular cellulose organization (Fig. 8, I and L). The *irx14* columellae either lacked rays or displayed cellulosic columns that were highly variable in width and height. However, unlike the *muci10* mutant, the *irx14* seeds had no obvious decreases in S4B signal intensity relative to the wild type (Fig. 8).

Several monoclonal antibodies were used to determine where RG I and xylan are located in the adherent mucilage layer, relative to cellulose counterstained with S4B (Fig. 9; Supplemental Fig. S7). Unbranched RG I, bound by CCRC-M36 (Young et al., 2008; Pattathil et al., 2010), was observed at the edge of wild-type mucilage capsules (Fig. 9A; Griffiths et al., 2014) but directly surrounded the cellulosic rays in *muci21* (Fig. 9E). CCRC-M30, which was raised against Arabidopsis mucilage, showed similar results (Supplemental Fig. S7). A large-scale ELISA data set (Pattathil et al., 2010) indicates that the CCRC-M139 antibody, unlike LM10, should be able to bind xylan in wild-type Arabidopsis mucilage. We successfully used CCRC-M139 to label adherent mucilage around wild-type and *muci21* seeds (Fig. 9, G–L). In accordance with the biochemical composition analysis (Table III), mucilage displayed less intense CCRC-M139 signals compared with RG I labeled by CCRC-M36. Although its precise epitope structure remains to be confirmed, CCRC-M139 can bind unbranched xylan with degrees of polymerization of at least 6 (Schmidt et al., 2015). CCRC-M139 epitopes

Table III. *Polysaccharide composition of total mucilage extracts*

The relative amount (mol %) of each polysaccharide was calculated based on the linkage analysis results in Table II.

Polysaccharide	Wild Type	*muci21-1*	*irx14-2*
Arabinan	0.87 ± 0.05	0.90 ± 0.02	0.90 ± 0.05
Type I arabinogalactan	0.37 ± 0.08	0.28 ± 0.02	0.30 ± 0.17
Type II arabinogalactan	2.20 ± 1.25	1.70 ± 0.28	4.31 ± 2.53
Xylan	3.07 ± 0.20	1.42 ± 0.12[a]	0.35 ± 0.00[a]
Galactoglucomannan	1.79 ± 0.06	1.80 ± 0.17	1.64 ± 0.35
RG I	66.59 ± 1.27	65.02 ± 3.45	65.55 ± 2.22
HG	20.59 ± 2.28	22.22 ± 1.62	24.01 ± 0.04
Cellulose	0.56 ± 0.03	0.48 ± 0.12	0.47 ± 0.00[a]
Others	3.95 ± 1.68	6.17 ± 4.29	2.47 ± 0.40

[a]Significant difference (Student's *t* test, $P < 0.05$) from the wild type.

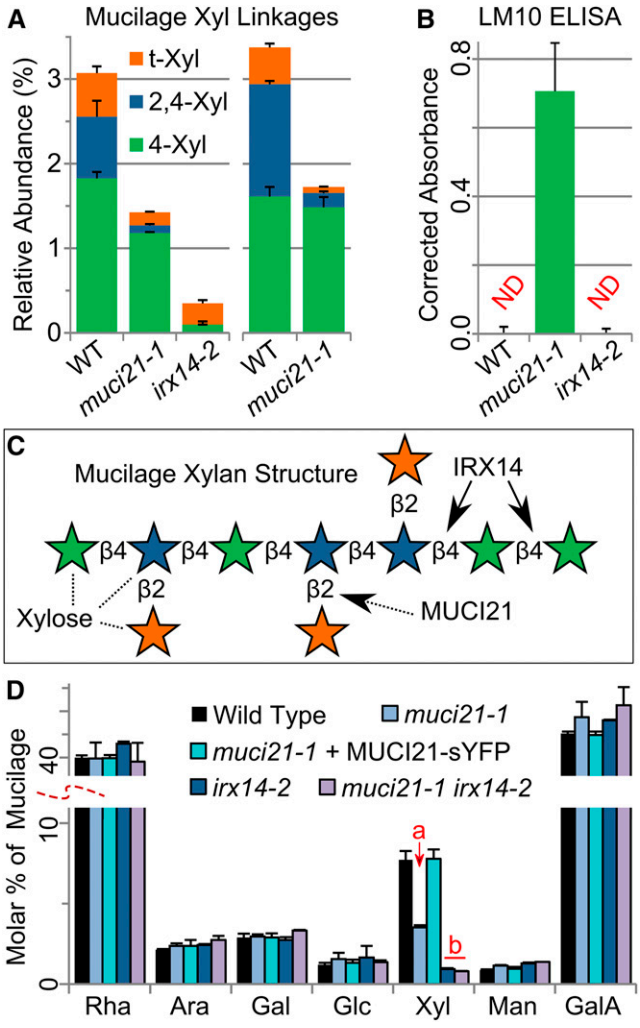

Figure 4. MUCI21 decorates xylan backbones produced by IRX14. A, Mucilage Xyl linkages from two independent experiments. B, Abundance of unbranched xylan labeled by LM10 (McCartney et al., 2005) in mucilage extracts. Epitopes were not detected (ND) in the wild type (WT) and *irx14* after background correction. C, Proposed structure of mucilage xylan, with Xyl units colored according to the legend in A. D, Composition of total mucilage extracts. Letters show that *35S:MUCI21-sYFP* rescued the Xyl defect of *muci21-1*, while *muci21 irx14* double mutants were similar to *irx14* (Student's *t* test, $P < 10^{-3}$). Data show means + SD of at least three biological replicates, except only two for *irx14-2* in A and the double mutant in D.

were only detected at the outer edge of wild-type adherent mucilage (Fig. 9J) but were more abundant in the *muci21* mutant and tightly surrounded the cellulosic rays (Fig. 9K), similar to the RG I distribution (Fig. 9E). In contrast to both the wild type and *muci21*, no pectin or xylan was detected at the surface of *irx14* seeds (Fig. 9). The irregular cellulosic columns observed in *irx14* seeds stained directly with S4B (Fig. 8L) were detached by the washes of the immunolabeling procedure (Fig. 9, F and L). These data suggests that while xylan branches added by MUCI21 are primarily required to anchor the pectic components of mucilage to the seed surface, a certain amount of the xylan backbone produced by IRX14 is necessary for maintaining the architecture of the cellulose.

DISCUSSION

Mucilage Contains Hemicelluloses Typical of Secondary Walls

Even though Arabidopsis seed mucilage consists primarily of unbranched RG I, there is mounting evidence that it also contains several polysaccharides found in typical secondary walls (Voiniciuc et al., 2015b). In spite of their low abundance, these minor components are important for the overall architecture and properties of the mucilage capsule. For example, cellulose is essential for the adherence of mucilage to the seed (Harpaz-Saad et al., 2011; Mendu et al., 2011; Sullivan et al., 2011; Griffiths et al., 2015), while galactoglucomannan is indispensable for the density of pectic polymers and the structure of cellulose (Voiniciuc et al., 2015a). Based on labeling with anti-XyG polyclonal antibody, whose cross-reactivity to other hemicelluloses remains unclear (Young et al., 2008), and the detection of linkages typical of branched xylan, two other hemicelluloses could occur in Arabidopsis seed mucilage (Haughn and Western, 2012; Voiniciuc et al., 2015b). We investigated xylan and XyG presence and functions by characterizing the mucilage phenotypes of mutants deficient in these hemicelluloses (Supplemental Table S1). The severe mucilage defects caused by three independent insertions in

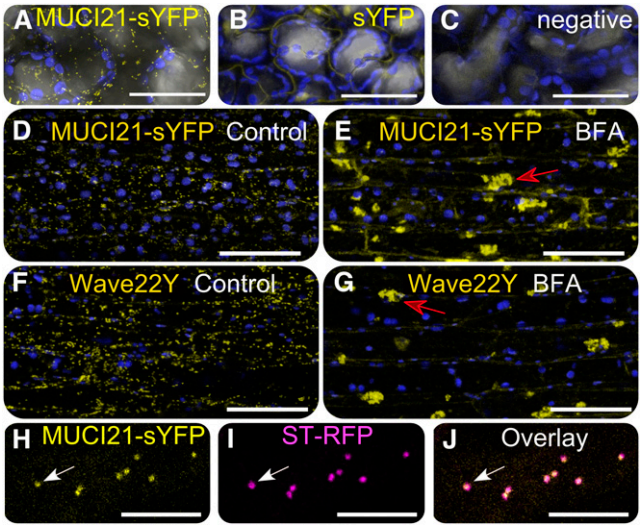

Figure 5. MUCI21-sYFP proteins are localized in the Golgi. Arabidopsis cells expressing MUCI21-sYFP (A), the free sYFP tag (B), or no transgene (C). A to C, sYFP (yellow), chloroplast intrinsic fluorescence (blue), and transmitted light (gray) signals overlaid in Fiji. E to H, After BFA treatment, MUCI21-sYFP and the Wave22Y Golgi marker aggregated in large bodies (red arrows). H to J, MUCI21-sYFP and ST-RFP Golgi punctae colocalized (white arrows). Bars = 50 (A–G) and 10 μm (H–J).

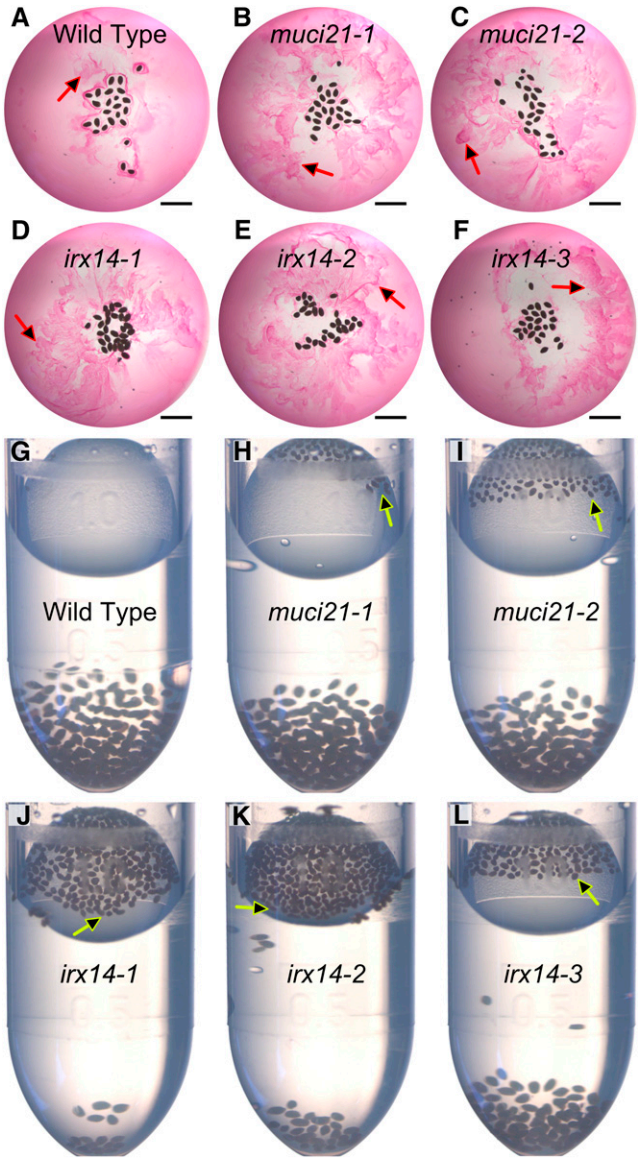

Figure 6. Mucilage is easily detached from *muci21* and *irx14* seeds. A to F, Nonadherent mucilage (arrows) released by seeds hydrated directly in RR. G to L, The majority of *irx14* seeds, and some *muci21* seeds, floated (arrows) after 20 min of contact with water. Similar seed quantities were added to each tube. Bars = 2 mm.

IRX14 (Figs. 3 and 4), an essential player for xylan elongation (Brown et al., 2007; Lee et al., 2010; Wu et al., 2010; Mortimer et al., 2015), demonstrate that xylan represents the main Xyl-rich polymer in mucilage and that its structure is critical for mucilage attachment to seeds. By contrast, our analysis of five *xxt* single mutants and the *xxt1;2;5* triple mutant (Supplemental Fig. S3), which lacks detectable XyG in all other Arabidopsis tissues examined (Zabotina et al., 2012), indicates that this polysaccharide is either absent or not essential for mucilage structure. We therefore conclude that heteromannans and xylans are the most abundant hemicelluloses in seed mucilage, similar to other secondary walls (Scheller and Ulvskov, 2010).

MUCI21, a GT61 Protein, Decorates Xylan with Unusual Side Chains

Through coexpression analysis with known mucilage genes, we have identified a new player that is essential for xylan biosynthesis. *MUCI21* encodes a member of GT61 clade B, whose biological functions were previously unknown (Fig. 1). MUCI21 is, to our knowledge, the first Arabidopsis GT61 to be characterized, and our data indicates that it plays critical roles in the substitution of xylan in SCE cells. Golgi-localized MUCI21-sYFP proteins fully rescued the Xyl deficiency and the RR staining defects of *muci21* mutants but not those of the *irx14* mutant (Figs. 3 and 4D). Consistent with MUCI21 only facilitating the substitution and not the elongation of xylan (Fig. 4C), 4-Xyl (unbranched xylan backbone) levels were not significantly reduced in both of our two independent analyses of glycosyl linkages in *muci21* mucilage (Table II; Supplemental Table S3). However, the severe loss of branched 2,4-Xyl units in the *muci21* mutant did not cause a proportional increase in 4-Xyl linkages (Fig. 4A). This suggests that in contrast to decoration of stem glucuronoxylan by GUX proteins (Mortimer et al., 2010; Lee et al., 2012a), mucilage xylan substitution by MUCI21 is not completely uncoupled from the elongation of the xylan backbone by IRX14. This implies that MUCI21 may function in cooperation with other biosynthetic enzymes, as proposed for some GT61 proteins in grasses (Faik et al., 2014). This scenario could explain why purified MUCI21 proteins did not show any XylT activity. Consistent with the role of IRX14 in xylan elongation in other Arabidopsis stems (Brown et al., 2007; Lee et al., 2010; Wu et al., 2010; Mortimer et al., 2015), the *muci21 irx14* double mutant phenocopied the reduced Xyl content of *irx14* single mutants (Fig. 4D).

Although we were unable to confirm the predicted XylT activity of MUCI21 proteins in vitro using *E. coli* or *N. benthamiana* expression systems, this biochemical activity has already been reported for two other GT61 proteins. The related XYLT and XAX enzymes, from clades A and C (Fig. 1) catalyze the transfer of β-1,2-Xyl units onto different substrates: *N*-glycoproteins and arabinoxylan (Strasser et al., 2000; Chiniquy et al., 2012), respectively. Two independent glycosyl linkage analyses of wild-type and *muci21* mucilage extracts revealed no consistent changes in Ara linkages but identified proportional decreases in t-Xyl and 2,4-Xyl units (Table II; Supplemental Table S3). This suggests that mucilage xylan is primarily decorated with Xyl residues (Fig. 4C). Because some groups detected trace levels of 3,4-Xyl (Dean et al., 2007; Arsovski et al., 2009; Huang et al., 2011), which could be substituted with 3-Ara units, a minor domain of mucilage xylan could have side chains distinct from the model shown in Figure 4C. Even though *MUCI21* is specifically

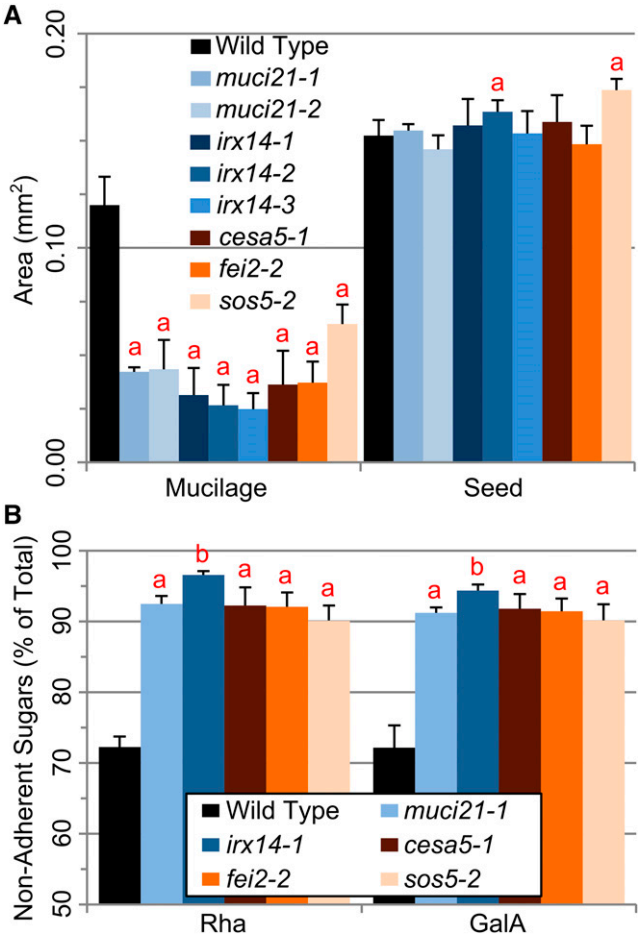

Figure 7. Comparison of *muci21* and *irx14* with other loss-of-adherence mutants. A, Dimensions of seeds and their RR-stained mucilage capsules. B, Rha and GalA easily detached from the mutant seeds. Data show means + SD of five biological replicates. The a and b indicate significant changes between the wild type and the mutants (Student's *t* test, $P < 0.05$).

expressed in the seed coat (Fig. 2), and the highly branched xylan observed in mucilage has not been previously reported, glucuronoxylan in other Arabidopsis tissues could also be decorated with a few t-Xyl units. This would be difficult to notice in stem alcohol-insoluble residues, because such extracts contain both primary and secondary walls, and t-Xyl units would be typically assigned to XyG (Pettolino et al., 2012). Conversely, mucilage cannot be frequently substituted with GlcA because there are only trace amounts of this sugar in mucilage extracts (Voiniciuc et al., 2015b), and *gux1* and *gux2* mutants had normal mucilage properties (Supplemental Fig. S3). Mucilage xylan probably has a unique structure that has not been previously described (Fig. 4C). Because this polymer represents only approximately 0.1% of wild-type dry seeds (Table I), its purification and characterization is not trivial. Future studies should elucidate the precise structure of xylan in mucilage and in other seed tissues, where xylan biosynthetic genes are also expressed (Supplemental Fig. S1).

Defects in Two Distinct Mucilage Properties Can Cause Seed Flotation

The detachment of mucilage from both *muci21* and *irx14* mutant seeds is significantly higher than in the wild type (Figs. 3 and 7), indicating the importance of xylan polysaccharides for the architecture of this specialized wall. In the *irx14* mutant, the mucilage detachment was so severe that most seeds did not sink even after prolonged contact with water (Fig. 6), similar to floating mucilage-releasing (FMR) natural Arabidopsis accessions (Saez-Aguayo et al., 2014). The gene(s) responsible for the FMR defects remain unknown but were predicted to be involved in cellulose production (Saez-Aguayo et al., 2014). Our results demonstrate that the FMR phenotype could also be caused by impaired xylan synthesis, rather than a direct loss of cellulose. In addition to these severe loss-of-adherence mutants, seed flotation may also be triggered by reduced mucilage release from SCE cells. Mutations in at least nine different genes impair mucilage release (Voiniciuc et al., 2015b), primarily by altering the content or decorations

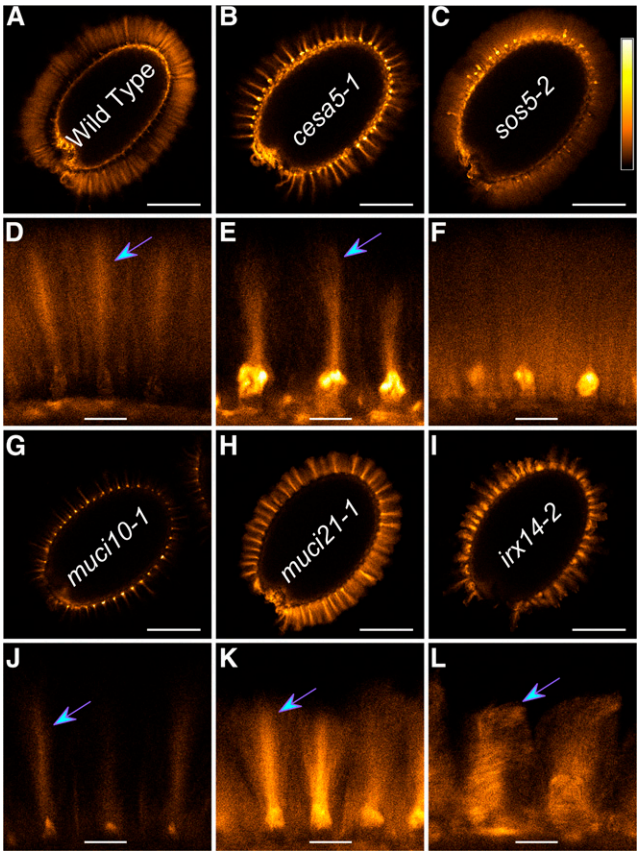

Figure 8. Cellulose structure in mutants with impaired mucilage adherence. A to L, S4B staining of cellulose in mucilage. Signals were visualized with the Orange Hot look-up table, using the calibration bar shown in C. All mutants displayed ray-like regions (arrows) except *sos5*. Magnified panels correspond to the seeds above them. Bars = 200 (A–C and G–I) and 25 μm (D–F and J–L).

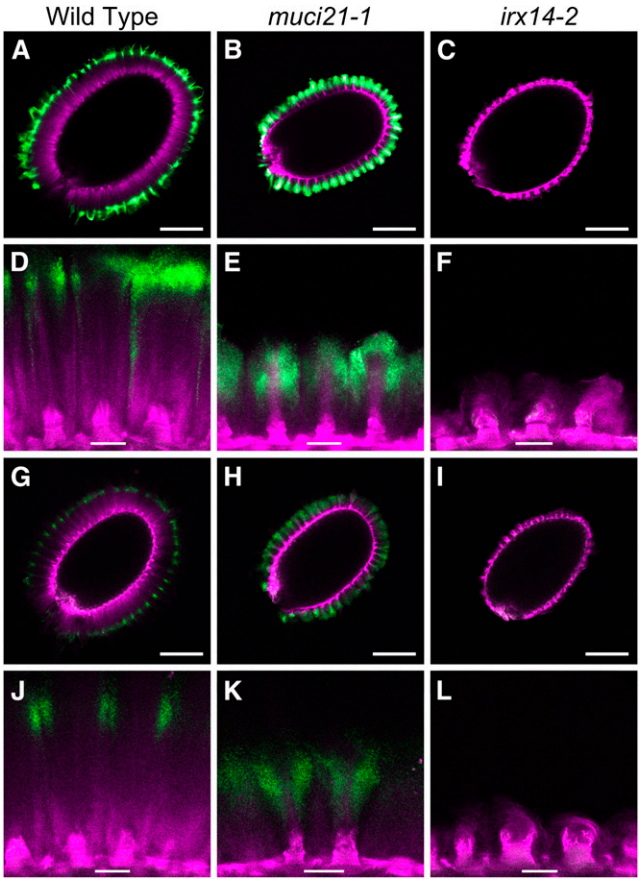

Figure 9. *muci21* and *irx14* mucilage has impaired RG I and xylan distribution. Optical sections show unbranched RG I labeled by CCRC-M36 (A–F) or xylan bound by CCRC-M139 (G–L) in green. Cellulose was counterstained with S4B (magenta). As xylan epitopes were less abundant than RG I, green intensity was increased in postacquisition (G–L). Bars = 200 (A–C and G–I) and 25 μm (D–F and J–L).

of pectin polymers. For example, mucilage release is prevented by increased RG I branching (Dean et al., 2007; Macquet et al., 2007; Arsovski et al., 2009) or by a lower degree of pectin methylesterification (Rautengarten et al., 2008; Saez-Aguayo et al., 2013). Although distinct defects in the release and the attachment of mucilage cause natural variants to float, and might improve seed dispersal over rivers (Saez-Aguayo et al., 2014), the exact advantage of each of mechanism has not been investigated.

Mucilage Adherence Is Maintained by Multiple Polymers

Xylan likely mediates pectin attachment in cooperation with other polysaccharides and glycoproteins. Multiple groups previously showed that cellulose, organized in ray-like structures, is essential for anchoring RG I polymers to the seed surface (Harpaz-Saad et al., 2011; Mendu et al., 2011; Sullivan et al., 2011; Griffiths et al., 2014, 2015; Ben-Tov et al., 2015). The main biological function of hemicelluloses is to strengthen the cell wall via interactions with cellulose (Scheller and Ulvskov, 2010). Based on *muci10* mucilage defects and the dramatic effects of α-galactosidase and β-mannanase digestion on pectin attachment, galactoglucomannan primarily maintains the structure of cellulose but is also partially required to anchor pectin (Voiniciuc et al., 2015a). Unlike *muci10*, the *muci21* mutant had surprisingly normal cellulose distribution (Fig. 8) but had RG I detachment defects as severe as the *cesa5* cellulose mutant (Fig. 7). The nearly complete loss of xylan in the *irx14* mutant further reduced mucilage attachment (Fig. 7B) and disrupted the uniform distribution of the cellulosic rays (Fig. 8). These data, together with the in situ colocalization of RG I and xylan epitopes around the cellulosic rays (Fig. 9), suggest that mucilage xylan, via its frequent branches, may function as an intermediate linker between RG I polymers and cellulose microfibrils. In agreement with the normal xylem morphology of *gux1 gux2* stems (Mortimer et al., 2010), our results indicate that cellulose organization is only severely disrupted by reduced xylan elongation (*irx14* mutant) and not by decreased substitution (*muci21* mutant).

In addition to the hemicellulose-cellulose network, adherence of mucilage to seeds is affected by two surface proteins, SOS5 and FEI2, as well as by the structure of pectin itself. Mucilage adherence is positively regulated by the HG degree of methylesterification (Voiniciuc et al., 2013). The presence of too much unesterified pectin can completely block the release of mucilage from the seed (Rautengarten et al., 2008; Saez-Aguayo et al., 2013). In contrast to the known pectin methylesterification mutants, the *muci21* and *irx14* mucilage defects were not affected by the presence of Ca^{2+} ions, consistent with our biochemical data that the increased detachment results from the specific loss of xylan rather than from pleiotropic changes in HG structure (Tables I and III). The roles of SOS5 and FEI2 are even less clear than those of the polysaccharides described above. These proteins were initially proposed to function in a linear pathway that regulates the CESA5-mediated synthesis of cellulose in mucilage (Harpaz-Saad et al., 2011). However, detailed phenotypic analyses of *sos5* and *cesa5* single and double mutants demonstrate that the affected players mediate adherence via partially independent mechanisms (Griffiths et al., 2014). Because RG I and xylan can be covalently linked via an arabinogalactan protein (Tan et al., 2013), it is tempting to speculate that SOS5, which is likely glycosylated (Basu et al., 2015), could be a structural component of such a complex in mucilage. Alternatively, RG I polymers could be directly linked to xylans (Naran et al., 2008; Tan et al., 2013; Cornuault et al., 2015), which could interact with cellulose microfibrils via hydrogen bonding. Because Arabidopsis mucilage attachment appears to be a complex trait, controlled by many genes, the roles of the different players should be further dissected by analysis of double mutants (Griffiths et al., 2014) or biochemical means (Tan et al., 2013). Mucilage provides a good model system to explore how xylans interact with other polymers to control the architecture of the cell wall.

Arabidopsis SCE Cells Are Excellent to Explore Xylan Biosynthesis

Surprisingly, only *IRX14* plays nonredundant roles in the elongation of mucilage xylan, while knockout mutations in *IRX9* and *IRX10*, two other promising *MUCI* candidates, did not disrupt the properties or Xyl content of mucilage. This could be caused by the presence of functional redundant *IRX9-L* and *IRX10-L* in developing seed coats, although they are not specifically associated with mucilage production (Supplemental Figs. S1 and S2). Our results show that Arabidopsis SCE cells offer an exciting new platform to explore the molecular mechanisms for the elongation and substitution of xylan. Although psyllium mucilage has more abundant levels of heteroxylan, it likely evolved to have a xylan synthase complex without GT43 proteins that is distinct from monocots as well as other dicots (Jensen et al., 2013). Therefore, Arabidopsis seed mucilage represents a better model to test the functions of genes required for xylan synthesis. In addition, our functional characterization of *MUCI21* suggests that GT61 clade B proteins are involved in xylan substitution, similar to clade A members (Fig. 1). This discovery increases the arsenal of genes that could be used to manipulate the structure of this abundant hemicellulose for improved nutrition or feedstocks.

MATERIALS AND METHODS

Plant Material

The insertion mutants analyzed in this study are listed in Supplemental Table S1, and were selected from the SALK (Alonso et al., 2003), SAIL (Sessions et al., 2002), WiscDsLox (Woody et al., 2007), and GABI-Kat (Kleinboelting et al., 2012) collections, using the T-DNA Express tool (http://signal.salk.edu/cgi-bin/tdnaexpress). Seeds were obtained from the Nottingham Arabidopsis Stock Centre (http://arabidopsis.info). Plants were grown as previously described (Voiniciuc et al., 2015a, 2015b) in individual $7 \times 7 \times 8$-cm pots at constant light (around 170 μE m^{-2} s^{-1}), temperature (20°C), and relative humidity (60%). Seeds from each plant were harvested into individual paper bags. Plants were genotyped by Touch-and-Go PCR (Berendzen et al., 2005), with the primers listed in Supplemental Table S4. These were created using the SALK T-DNA Primer Design (http://signal.salk.edu/tdnaprimers.2.html).

Phylogenetic Analysis

All the MUCI21-related GT61 protein sequences from five organisms were obtained using the standard protein BLAST provided by National Center for Biotechnology Information. These data were used to build phylogenetic analysis in the MEGA6.0 software (http://www.megasoftware.net/; Tamura et al., 2013) using a published guide (Hall, 2013). Proteins were aligned (MUSCLE method), and the evolutionary history was inferred using the maximum-likelihood method. The tree was built using the best substitution model found (LG + G) and partial deletion of gaps/missing data. Its reliability was tested with the bootstrap method (1,000 replicates). The three GT61 clades were named as first reported (Anders et al., 2012). Proteins that did not cluster with these clades were excluded from the phylogenetic analysis.

RNA Isolation and qRT-PCR Analysis

Developing siliques were staged and harvested as previously described (Voiniciuc et al., 2015a). For Figure 2C, RNA was isolated using the ZR Plant RNA MiniPrep kit (Zymo Research). For Figure 2D, RNA was isolated with the RNeasy Plant Mini Kit (Qiagen). The on-column DNase I treatment recommended by the manufacturers was performed for all samples to remove any DNA contaminants. RNA was quantified using a NanoDrop 1000 (Thermo Fisher Scientific) and the Qubit RNA High Sensitivity kit (Thermo Fisher Scientific). First-strand complementary DNA (cDNA) was synthesized using the iScript cDNA Synthesis Kit (Bio-Rad) and 200 ng of RNA template. The primers for qRT-PCR amplification (Supplemental Table S4) were designed using the QuantPrime (http://www.quantprime.de) tool (Arvidsson et al., 2008). *UBQ5* served as a reference gene (Gutierrez et al., 2008). The amplicons were detected using iQ SYBR Green Supermix (Bio-Rad) and a Bio-Rad MyiQ system. Amplification efficiencies, determined using a serial dilution of DNA or cDNA, were used to calculate fold changes in gene expression (Pfaffl, 2001; Fraga et al., 2008).

Mucilage RR Staining

Except for the seed floatation experiment (Fig. 6, G–L), all seeds were hydrated for 5 min in water and stained for 5 min with 0.01% (w/v) RR (VWR International) in 24-well plates, as previously described in detail (Voiniciuc et al., 2015a). Every well was then imaged with a Leica DFC 295 camera on a Leica MZ12 stereomicroscope. Nonadherent mucilage was examined by adding dry seeds to 300 μL of 0.01% (w/v) RR solution (Fig. 6, A–F). The effect of calcium cross-links on mucilage properties was investigated by hydrating seeds in 500 μL of water, 50 mM $CaCl_2$, or 50 mM EDTA, pH 9.5, for 60 min at 125 rpm in a 24-well plate. Seeds were rinsed twice with water and then stained with RR. All images in this study were processed in Fiji (http://fiji.sc/Fiji; Schindelin et al., 2012).

Quantification of Mucilage Area

Mucilage and seed dimensions were quantified in Fiji using a published protocol (Voiniciuc et al., 2015a), with the following updates. Mucilage plus seed regions were segmented using these color thresholding (minimum, maximum) parameters: red (0, 255), green (0, 135), and blue (0, 255), while seed regions were segmented using red (0, 145), green (0, 255), and blue (0, 255). Regions of interest were selected using the Analyze Particles function (circularity = 0.5–1.0), excluding edges and extreme particle sizes.

Statistical Analyses

The dimensions of mucilage capsules and their biochemical composition (see detailed methods below) were normally distributed according to the Shapiro-Wilk test (Shapiro and Wilk, 1965), performed using the Real Statistics Resource Pack (http://www.real-statistics.com) for Microsoft Excel 2010. Statistically significant changes were identified through the T.TEST function in Microsoft Excel 2010, using two-tailed distribution and assuming equal variance of two samples.

Mucilage Monosaccharide Composition

Total mucilage was extracted from seeds, and its monosaccharide composition was analyzed as previously described in detail (Voiniciuc et al., 2015a). In summary, 5 mg of seeds was vigorously mixed with 1 mL of water, spiked with ribose as internal standard, using a ball mill (Retsch MM400) for 30 min at 30 Hz. The seeds were allowed to settle, and the supernatant was transferred to a new tube, dried, and then hydrolyzed using 2 N trifluoroacetic acid for 90 min. After evaporating the trifluoroacetic acid, monosaccharides were resuspended in water and were quantified by high-performance anion-exchange chromatography (HPAEC) with pulsed amperometric detection (PAD) using a Dionex system equipped with a CarboPac PA20 column and GP50, ED50, and AS50 modules. Amounts were normalized to the internal standard and quantified using standard calibration curves. Figures 4D and 7B and Supplemental Table S2 results were obtained in parallel with analyses of *muci10* mutants (Voiniciuc et al., 2015a) and share the same reference wild-type values. For each data set, all genotypes were grown, harvested, processed, and analyzed simultaneously. Nonadherent (with ribose as internal standard) and adherent mucilage (with 2-deoxy-D-Glc as internal standard) fractions were sequentially extracted as previously described (Voiniciuc et al., 2015a).

Glycosyl Linkage Analysis of Seed Mucilage

Total mucilage was extracted using the ball mill method and prepared for linkage analysis via a previously published protocol (Voiniciuc et al., 2015a), including the following key steps. An aliquot of the extracted mucilage was

used for HPAEC-PAD monosaccharide analysis. The remaining sample was acidified, and uronic acids were reduced to their respective 6,6-dideuterio derivatives (Gibeaut and Carpita, 1991). Afterward, the samples were extensively dialyzed against water, lyophilized, and solubilized in anhydrous dimethyl sulfoxide (DMSO). The polysaccharides were methylated (Gille et al., 2009), hydrolyzed, derivatized to the corresponding alditol acetates, and analyzed by gas chromatography-mass spectrometry (Foster et al., 2010), using sodium borodeuteride for the reduction. For Supplemental Table S3, the *muci21-1* results were obtained in parallel with the analysis of *muci10* (Voiniciuc et al., 2015a) and share the same reference wild-type values. Polysaccharide composition was calculated using an existing protocol (Pettolino et al., 2012), with minor modifications. The 2,3-Rha, 2,4-GalA, and 4,6-GalA linkages were assigned to RG I, and t-Xyl was assigned to xylan.

LM10 ELISA of Mucilage Xylan

ELISA was performed as described (Pattathil et al., 2010), with minor modifications (Voiniciuc et al., 2015a). Total mucilage was extracted from 8 mg of seeds using 1 mL of water, and 125-μL aliquots of the supernatant were transferred to a 96-well plate (Corning). Based on our monosaccharide data, these aliquots yield 0.5 μg of Xyl, which should be sufficient to saturate the wells with xylan antigens. The LM10 antibody for unbranched or low-substituted xylan (McCartney et al., 2005) was obtained from PlantProbes (http://www.plantprobes.net).

Stem Monosaccharide Composition

Alcohol-insoluble residue isolated from the main inflorescence stem (bottom 3 cm) of 4-week-old Arabidopsis (*Arabidopsis thaliana*) plants was processed for monosaccharide composition analysis with HPAEC-PAD, as previously described (Voiniciuc et al., 2015a). For Supplemental Figure S4B, the *muci21* results were obtained in parallel to the analysis of *muci10* (Voiniciuc et al., 2015a) and share the same reference wild-type values.

Mucilage Cellulose Staining

Around 20 seeds were hydrated in 500 μL of water in a 24-well plate for 5 min. The water was removed, and cellulose was stained with 0.01% (w/v) S4B (now sold as Direct Red 23 [Sigma-Aldrich]) in 50 mM NaCl solution. After 60 min at 125 rpm, the seeds were rinsed three times with 300 μL of water and imaged with the Leica SP8 confocal system (552-nm excitation and 600- to 650-nm emission).

Whole-Seed Immunolabeling

For immunolabeling, the four CCRC primary antibodies used were obtained from CarboSource (http://www.ccrc.uga.edu/~carbosource/CSS_home.html), while Alexa Fluor 488 goat anti-mouse secondary antibody was purchased from Life Technologies. Samples were prepared in a 24-well plate, and all incubations were performed on horizontal shaker (125 rpm, room temperature) for the indicated duration. For each sample, around 20 seeds were incubated in 500 μL of water for 30 min. After removing 470 μL of water from each well, seed mucilage was blocked for 30 min with 100 μL of 5% (w/v) bovine serum albumin (BSA) in phosphate-buffered saline (PBS; pH 7.0) solution. The blocking solution was removed, and seeds were sequentially incubated for 90 min with primary and secondary antibodies diluted 1:10 and 1:100, respectively, using 1% (w/v) bovine serum albumin in PBS solution. The seeds were washed five times with 300 μL of PBS after each antibody treatment. Seeds were counterstained for 30 min with 0.01% (w/v) S4B in 100 mM NaCl, rinsed four times with water, and stored overnight at 4°C. Images were acquired on a Leica SP8 confocal microscope using the following settings: Alexa Fluor signal (488-nm excitation and 500- to 530-nm emission) and S4B signal (552-nm excitation and 590- to 700-nm emission). Wild-type samples prepared without the primary antibody and/or S4B served as negative controls.

Expression and Analysis of MUCI21-sYFP Proteins

The *35S:MUCI21-sYFP* construct was created using the pCV01 vector (Voiniciuc et al., 2015a). Genomic DNA was isolated using a commercial kit (GeneON). A 1,677-bp *MUCI21* fragment (the complete coding sequence, without the stop codon) was amplified using Phusion High-Fidelity DNA Polymerase (New England Biolabs). Because the primers had large adapters (Supplemental Table S4), we first used five three-step amplification cycles with a low annealing temperature (55°C), followed by 30 two-step Phusion PCR cycles with an annealing/extension temperature of 72°C. The gel-purified fragment was then prepared for ligation-independent cloning as described (De Rybel et al., 2011). The plasmid was verified by Sanger sequencing and, using *Agrobacterium tumefaciens* GV3101::pMP90::pSOUP cells, was transformed in Arabidopsis plants using a modified floral spray method (Weigel and Glazebrook, 2006), with an infiltration medium containing 5% (w/v) Suc and 0.02% (v/v) Silwet L-77. T1 seedlings were selected with a 10 mg L^{-1} glufosinate-ammonium spray (Sigma-Aldrich).

Protein subcellular localization in rosette leaf epidermal cells was examined using a Leica SP8 confocal microscope. For the BFA treatment, seeds were placed on one-half-strength Murashige and Skoog plates (Voiniciuc et al., 2015b). After 6 d under constant light, seedlings were transferred to a 24-well plate and incubated (60 min at 80 rpm) with 0.02% (v/v) DMSO (negative control) or 100 μg mL^{-1} BFA (Sigma Aldrich) in 0.02% (v/v) DMSO. Hypocotyl epidermal cells were imaged using a Leica SP8 confocal microscope. The sYFP signal (500- to 575-nm emission) and intrinsic plant fluorescence (615- to 705-nm emission) were simultaneously acquired using 488-nm laser excitation.

Expression and Analysis of GST-MUCI21 Proteins

The MUCI21 protein topology was assessed using ARAMEMNON (Schwacke et al., 2003). A truncated *MUCI21* (1,290-bp) fragment, without the 5′ region encoding a transmembrane span, was amplified from cDNA, using the primers in Supplemental Table S4. The amplicon was inserted between the *Not*I and *Sal*I sites of the pGEX-5x-3 vector (GE Healthcare) to generate an N-terminal fusion to GST. Plasmids were propagated in NEB 5-α *Escherichia coli* (New England Biolabs) and, after sequence verification, were transformed in BL21(DE3) *E. coli* (New England Biolabs) cells for protein expression. Proteins were expressed and purified precisely as described (Voiniciuc et al., 2015a). XylT activity was assayed with the UDP-Glo Glycosyltransferase Assay (Promega, Custom Assay CS1681A05), according to the manufacturer's instructions and the conditions that were successful for the IRX10-L xylan XylT (Urbanowicz et al., 2014). GT reactions (25 μL) containing 50 mM HEPES-NaOH buffer (pH 7.0) and 1.25 μg of purified protein were carried out using 800 μM ultrapure UDP-Xyl (CarboSource) as donor and 1 mM of an acceptor substrate: xylobiose, xylotriose, xylotetraose, xylopentaose, xylohexaose, or cellohexaose (all from Megazyme International Ireland) or RG I oligosaccharides. GT reactions were incubated for 60 min at 23°C in a 96-well plate (VWR International). After adding 25 μL of UDP-Glo detection reagent and incubation for 60 min at 23°C, luminescence was measured with a Synergy H1M Hybrid Reader (BioTek) and quantified using a serial dilution of UDP standards (Promega).

Supplemental Data

The following supplemental materials are available.

Supplemental Figure S1. Xylan gene expression in developing seeds.

Supplemental Figure S2. Gene expression in seeds and seed coats.

Supplemental Figure S3. Mutants with normal mucilage properties.

Supplemental Figure S4. Cell wall composition of stems.

Supplemental Figure S5. XylT assays for *E.coli*-purified proteins.

Supplemental Figure S6. Effects of Ca^{2+} on mucilage defects.

Supplemental Figure S7. CCRC-M30 labeling of mucilage.

Supplemental Table S1. Mutants examined for mucilage defects.

Supplemental Table S2. *muci21* and *irx14* chemotypes are heritable.

Supplemental Table S3. Linkage analysis of *muci21-1* mucilage.

Supplemental Table S4. Primer sequences (5′–3′) used.

ACKNOWLEDGMENTS

We thank Dr. Berit Ebert and Dr. Henrik V. Scheller (Joint BioEnergy Institute) for performing the *N. benthamiana* XylT assay and Dr. Marie-Christine Ralet (Institut National de la Recherche Agronomique) for providing the pooled RG I oligosaccharides.

Received September 11, 2015; accepted October 17, 2015; published October 19, 2015.

LITERATURE CITED

Alonso JM, Stepanova AN, Leisse TJ, Kim CJ, Chen H, Shinn P, Stevenson DK, Zimmerman J, Barajas P, Cheuk R, et al (2003) Genome-wide insertional mutagenesis of *Arabidopsis thaliana*. Science **301:** 653–657

Anders N, Wilkinson MD, Lovegrove A, Freeman J, Tryfona T, Pellny TK, Weimar T, Mortimer JC, Stott K, Baker JM, et al (2012) Glycosyl transferases in family 61 mediate arabinofuranosyl transfer onto xylan in grasses. Proc Natl Acad Sci USA **109:** 989–993

Arsovski AA, Popma TM, Haughn GW, Carpita NC, McCann MC, Western TL (2009) AtBXL1 encodes a bifunctional β-D-xylosidase/α-L-arabinofuranosidase required for pectic arabinan modification in Arabidopsis mucilage secretory cells. Plant Physiol **150:** 1219–1234

Arvidsson S, Kwasniewski M, Riaño-Pachón DM, Mueller-Roeber B (2008) QuantPrime: a flexible tool for reliable high-throughput primer design for quantitative PCR. BMC Bioinformatics **9:** 465

Basu D, Wang W, Ma S, DeBrosse T, Poirier E, Emch K, Soukup E, Tian L, Showalter AM (2015) Two hydroxyproline galactosyltransferases, GALT5 and GALT2, function in arabinogalactan-protein glycosylation, growth and development in Arabidopsis. PLoS One **10:** e0125624

Belmonte MF, Kirkbride RC, Stone SL, Pelletier JM, Bui AQ, Yeung EC, Hashimoto M, Fei J, Harada CM, Munoz MD, et al (2013) Comprehensive developmental profiles of gene activity in regions and subregions of the Arabidopsis seed. Proc Natl Acad Sci USA **110:** E435–E444

Ben-Tov D, Abraham Y, Stav S, Thompson K, Loraine A, Elbaum R, De Souza A, Pauly M, Kieber JJ, Harpaz-Saad S (2015) COBRA-LIKE 2, a member of the GPI-anchored COBRA-LIKE family, plays a role in cellulose deposition in Arabidopsis seed coat mucilage secretory cells. Plant Physiol **167:** 711–724

Berendzen K, Searle I, Ravenscroft D, Koncz C, Batschauer A, Coupland G, Somssich IE, Ulker B (2005) A rapid and versatile combined DNA/RNA extraction protocol and its application to the analysis of a novel DNA marker set polymorphic between *Arabidopsis thaliana* ecotypes Col-0 and Landsberg *erecta*. Plant Methods **1:** 4

Bromley JR, Busse-Wicher M, Tryfona T, Mortimer JC, Zhang Z, Brown DM, Dupree P (2013) GUX1 and GUX2 glucuronyltransferases decorate distinct domains of glucuronoxylan with different substitution patterns. Plant J **74:** 423–434

Brown DM, Goubet F, Wong VW, Goodacre R, Stephens E, Dupree P, Turner SR (2007) Comparison of five xylan synthesis mutants reveals new insight into the mechanisms of xylan synthesis. Plant J **52:** 1154–1168

Brown DM, Zeef LAH, Ellis J, Goodacre R, Turner SR (2005) Identification of novel genes in *Arabidopsis* involved in secondary cell wall formation using expression profiling and reverse genetics. Plant Cell **17:** 2281–2295

Brown DM, Zhang Z, Stephens E, Dupree P, Turner SR (2009) Characterization of IRX10 and IRX10-like reveals an essential role in glucuronoxylan biosynthesis in Arabidopsis. Plant J **57:** 732–746

Chiniquy D, Sharma V, Schultink A, Baidoo EE, Rautengarten C, Cheng K, Carroll A, Ulvskov P, Harholt J, Keasling JD, et al (2012) XAX1 from glycosyltransferase family 61 mediates xylosyltransfer to rice xylan. Proc Natl Acad Sci USA **109:** 17117–17122

Cornuault V, Buffetto F, Rydahl MG, Marcus SE, Torode TA, Xue J, Crépeau MJ, Faria-Blanc N, Willats WG, Dupree P, et al (2015) Monoclonal antibodies indicate low-abundance links between heteroxylan and other glycans of plant cell walls. Planta **242:** 1321–1334

Cosgrove DJ (2005) Growth of the plant cell wall. Nat Rev Mol Cell Biol **6:** 850–861

De Rybel B, van den Berg W, Lokerse A, Liao CY, van Mourik H, Möller B, Peris CL, Weijers D (2011) A versatile set of ligation-independent cloning vectors for functional studies in plants. Plant Physiol **156:** 1292–1299

Dean G, Cao Y, Xiang D, Provart NJ, Ramsay L, Ahad A, White R, Selvaraj G, Datla R, Haughn G (2011) Analysis of gene expression patterns during seed coat development in Arabidopsis. Mol Plant **4:** 1074–1091

Dean GH, Zheng H, Tewari J, Huang J, Young DS, Hwang YT, Western TL, Carpita NC, McCann MC, Mansfield SD, et al (2007) The *Arabidopsis MUM2* gene encodes a β-galactosidase required for the production of seed coat mucilage with correct hydration properties. Plant Cell **19:** 4007–4021

Faik A, Jiang N, Held MA (2014) Xylan Biosynthesis in Plants, Simply Complex. Plants and BioEnergy. Springer New York, pp 153–181

Foster CE, Martin TM, Pauly M (2010) Comprehensive compositional analysis of plant cell walls (lignocellulosic biomass) part I: lignin. J Vis Exp **37:** e1745

Fraga D, Meulia T, Fenster S (2008) Real-time PCR. *In* SR Gallagher, EA Wiley, eds, Current Protocols: Essential Laboratory Techniques. John Wiley & Sons, New York, pp 1–33

Geldner N, Dénervaud-Tendon V, Hyman DL, Mayer U, Stierhof YD, Chory J (2009) Rapid, combinatorial analysis of membrane compartments in intact plants with a multicolor marker set. Plant J **59:** 169–178

Gibeaut DM, Carpita NC (1991) Tracing cell wall biogenesis in intact cells and plants: selective turnover and alteration of soluble and cell wall polysaccharides in grasses. Plant Physiol **97:** 551–561

Gille S, Hänsel U, Ziemann M, Pauly M (2009) Identification of plant cell wall mutants by means of a forward chemical genetic approach using hydrolases. Proc Natl Acad Sci USA **106:** 14699–14704

Griffiths JS, Šola K, Kushwaha R, Lam P, Tateno M, Young R, Voiniciuc C, Dean G, Mansfield SD, DeBolt S, et al (2015) Unidirectional movement of cellulose synthase complexes in Arabidopsis seed coat epidermal cells deposit cellulose involved in mucilage extrusion, adherence, and ray formation. Plant Physiol **168:** 502–520

Griffiths JS, Tsai AYL, Xue H, Voiniciuc C, Sola K, Seifert GJ, Mansfield SD, Haughn GW (2014) SALT-OVERLY SENSITIVE5 mediates Arabidopsis seed coat mucilage adherence and organization through pectins. Plant Physiol **165:** 991–1004

Gutierrez L, Mauriat M, Guénin S, Pelloux J, Lefebvre JF, Louvet R, Rusterucci C, Moritz T, Guerineau F, Bellini C, et al (2008) The lack of a systematic validation of reference genes: a serious pitfall undervalued in reverse transcription-polymerase chain reaction (RT-PCR) analysis in plants. Plant Biotechnol J **6:** 609–618

Hall BG (2013) Building phylogenetic trees from molecular data with MEGA. Mol Biol Evol **30:** 1229–1235

Harpaz-Saad S, McFarlane HE, Xu S, Divi UK, Forward B, Western TL, Kieber JJ (2011) Cellulose synthesis via the FEI2 RLK/SOS5 pathway and cellulose synthase 5 is required for the structure of seed coat mucilage in Arabidopsis. Plant J **68:** 941–953

Haughn GW, Western TL (2012) Arabidopsis seed coat mucilage is a specialized cell wall that can be used as a model for genetic analysis of plant cell wall structure and function. Front Plant Sci **3:** 64

Huang J, DeBowles D, Esfandiari E, Dean G, Carpita NC, Haughn GW (2011) The Arabidopsis transcription factor LUH/MUM1 is required for extrusion of seed coat mucilage. Plant Physiol **156:** 491–502

Jensen JK, Johnson N, Wilkerson CG (2013) Discovery of diversity in xylan biosynthetic genes by transcriptional profiling of a heteroxylan containing mucilaginous tissue. Front Plant Sci **4:** 183

Jensen JK, Johnson NR, Wilkerson CG (2014) *Arabidopsis thaliana* IRX10 and two related proteins from psyllium and *Physcomitrella patens* are xylan xylosyltransferases. Plant J **80:** 207–215

Jensen JK, Kim H, Cocuron JC, Orler R, Ralph J, Wilkerson CG (2011) The DUF579 domain containing proteins IRX15 and IRX15-L affect xylan synthesis in Arabidopsis. Plant J **66:** 387–400

Kajiura H, Okamoto T, Misaki R, Matsuura Y, Fujiyama K (2012) Arabidopsis β1,2-xylosyltransferase: substrate specificity and participation in the plant-specific *N*-glycosylation pathway. J Biosci Bioeng **113:** 48–54

Kleinboelting N, Huep G, Kloetgen A, Viehoever P, Weisshaar B (2012) GABI-Kat SimpleSearch: new features of the *Arabidopsis thaliana* T-DNA mutant database. Nucleic Acids Res **40:** D1211–D1215

Lee C, Teng Q, Huang W, Zhong R, Ye ZH (2010) The Arabidopsis family GT43 glycosyltransferases form two functionally nonredundant groups essential for the elongation of glucuronoxylan backbone. Plant Physiol **153:** 526–541

Lee C, Teng Q, Zhong R, Ye ZH (2012a) Arabidopsis GUX proteins are glucuronyltransferases responsible for the addition of glucuronic acid side chains onto xylan. Plant Cell Physiol **53:** 1204–1216

Lee C, Zhong R, Ye ZH (2012b) Arabidopsis family GT43 members are xylan xylosyltransferases required for the elongation of the xylan backbone. Plant Cell Physiol **53:** 135–143

Macquet A, Ralet MC, Loudet O, Kronenberger J, Mouille G, Marion-Poll A, North HM (2007) A naturally occurring mutation in an *Arabidopsis* accession affects a β-D-galactosidase that increases the hydrophilic potential of rhamnogalacturonan I in seed mucilage. Plant Cell **19:** 3990–4006

McCartney L, Marcus SE, Knox JP (2005) Monoclonal antibodies to plant cell wall xylans and arabinoxylans. J Histochem Cytochem **53:** 543–546

Mendu V, Griffiths JS, Persson S, Stork J, Downie AB, Voiniciuc C, Haughn GW, DeBolt S (2011) Subfunctionalization of cellulose synthases in seed coat epidermal cells mediates secondary radial wall synthesis and mucilage attachment. Plant Physiol **157:** 441–453

Mortimer JC, Faria-Blanc N, Yu X, Tryfona T, Sorieul M, Ng YZ, Zhang Z, Stott K, Anders N, Dupree P (2015) An unusual xylan in Arabidopsis primary cell walls is synthesised by GUX3, IRX9L, IRX10L and IRX14. Plant J **83:** 413–426

Mortimer JC, Miles GP, Brown DM, Zhang Z, Segura MP, Weimar T, Yu X, Seffen KA, Stephens E, Turner SR, et al (2010) Absence of branches from xylan in Arabidopsis gux mutants reveals potential for simplification of lignocellulosic biomass. Proc Natl Acad Sci USA **107:** 17409–17414

Mutwil M, Obro J, Willats WGT, Persson S (2008) GeneCAT: novel webtools that combine BLAST and co-expression analyses. Nucleic Acids Res **36:** W320–W326

Naran R, Chen G, Carpita NC (2008) Novel rhamnogalacturonan I and arabinoxylan polysaccharides of flax seed mucilage. Plant Physiol **148:** 132–141

Nebenführ A, Ritzenthaler C, Robinson DG (2002) Brefeldin A: deciphering an enigmatic inhibitor of secretion. Plant Physiol **130:** 1102–1108

North HM, Berger A, Saez-Aguayo S, Ralet MC (2014) Understanding polysaccharide production and properties using seed coat mutants: future perspectives for the exploitation of natural variants. Ann Bot (Lond) **114:** 1251–1263

Oikawa A, Lund CH, Sakuragi Y, Scheller HV (2013) Golgi-localized enzyme complexes for plant cell wall biosynthesis. Trends Plant Sci **18:** 49–58

Pattathil S, Avci U, Baldwin D, Swennes AG, McGill JA, Popper Z, Bootten T, Albert A, Davis RH, Chennareddy C, et al (2010) A comprehensive toolkit of plant cell wall glycan-directed monoclonal antibodies. Plant Physiol **153:** 514–525

Pettolino FA, Walsh C, Fincher GB, Bacic A (2012) Determining the polysaccharide composition of plant cell walls. Nat Protoc **7:** 1590–1607

Pfaffl MW (2001) A new mathematical model for relative quantification in real-time RT-PCR. Nucleic Acids Res **29:** e45

Rautengarten C, Usadel B, Neumetzler L, Hartmann J, Büssis D, Altmann T (2008) A subtilisin-like serine protease essential for mucilage release from Arabidopsis seed coats. Plant J **54:** 466–480

Ren Y, Hansen SF, Ebert B, Lau J, Scheller HV (2014) Site-directed mutagenesis of IRX9, IRX9L and IRX14 proteins involved in xylan biosynthesis: Glycosyltransferase activity is not required for IRX9 function in Arabidopsis. PLoS One **9:** e105014

Rennie EA, Hansen SF, Baidoo EE, Hadi MZ, Keasling JD, Scheller HV (2012) Three members of the Arabidopsis glycosyltransferase family 8 are xylan glucuronosyltransferases. Plant Physiol **159:** 1408–1417

Rennie EA, Scheller HV (2014) Xylan biosynthesis. Curr Opin Biotechnol **26:** 100–107

Rogowski A, Briggs JA, Mortimer JC, Tryfona T, Terrapon N, Lowe EC, Baslé A, Morland C, Day AM, Zheng H, et al (2015) Glycan complexity dictates microbial resource allocation in the large intestine. Nat Commun **6:** 7481

Saez-Aguayo S, Ralet MC, Berger A, Botran L, Ropartz D, Marion-Poll A, North HM (2013) PECTIN METHYLESTERASE INHIBITOR6 promotes *Arabidopsis* mucilage release by limiting methylesterification of homogalacturonan in seed coat epidermal cells. Plant Cell **25:** 308–323

Saez-Aguayo S, Rondeau-Mouro C, Macquet A, Kronholm I, Ralet MC, Berger A, Sallé C, Poulain D, Granier F, Botran L, et al (2014) Local evolution of seed flotation in Arabidopsis. PLoS Genet **10:** e1004221

Scheller HV, Ulvskov P (2010) Hemicelluloses. Annu Rev Plant Biol **61:** 263–289

Schindelin J, Arganda-Carreras I, Frise E, Kaynig V, Longair M, Pietzsch T, Preibisch S, Rueden C, Saalfeld S, Schmid B, et al (2012) Fiji: an open-source platform for biological-image analysis. Nat Methods **9:** 676–682

Schmidt D, Schuhmacher F, Geissner A, Seeberger PH, Pfrengle F (2015) Automated synthesis of arabinoxylan-oligosaccharides enables characterization of antibodies that recognize plant cell wall glycans. Chemistry **21:** 5709–5713

Schwacke R, Schneider A, van der Graaff E, Fischer K, Catoni E, Desimone M, Frommer WB, Flügge UI, Kunze R (2003) ARAMEMNON, a novel database for Arabidopsis integral membrane proteins. Plant Physiol **131:** 16–26

Sessions A, Burke E, Presting G, Aux G, McElver J, Patton D, Dietrich B, Ho P, Bacwaden J, Ko C, et al (2002) A high-throughput *Arabidopsis* reverse genetics system. Plant Cell **14:** 2985–2994

Shapiro SS, Wilk MB (1965) An analysis of variance test for normality (complete samples). Biometrika **52:** 591–611

Somerville C, Bauer S, Brininstool G, Facette M, Hamann T, Milne J, Osborne E, Paredez A, Persson S, Raab T, et al (2004) Toward a systems approach to understanding plant cell walls. Science **306:** 2206–2211

Strasser R, Mucha J, Mach L, Altmann F, Wilson IB, Glössl J, Steinkellner H (2000) Molecular cloning and functional expression of β1,2-xylosyltransferase cDNA from *Arabidopsis thaliana*. FEBS Lett **472:** 105–108

Sullivan S, Ralet MC, Berger A, Diatloff E, Bischoff V, Gonneau M, Marion-Poll A, North HM (2011) CESA5 is required for the synthesis of cellulose with a role in structuring the adherent mucilage of Arabidopsis seeds. Plant Physiol **156:** 1725–1739

Tamura K, Stecher G, Peterson D, Filipski A, Kumar S (2013) MEGA6: Molecular Evolutionary Genetics Analysis version 6.0. Mol Biol Evol **30:** 2725–2729

Tan L, Eberhard S, Pattathil S, Warder C, Glushka J, Yuan C, Hao Z, Zhu X, Avci U, Miller JS, et al (2013) An *Arabidopsis* cell wall proteoglycan consists of pectin and arabinoxylan covalently linked to an arabinogalactan protein. Plant Cell **25:** 270–287

Urbanowicz BR, Peña MJ, Moniz HA, Moremen KW, York WS (2014) Two Arabidopsis proteins synthesize acetylated xylan in vitro. Plant J **80:** 197–206

Voiniciuc C, Dean GH, Griffiths JS, Kirchsteiger K, Hwang YT, Gillett A, Dow G, Western TL, Estelle M, Haughn GW (2013) Flying saucer1 is a transmembrane RING E3 ubiquitin ligase that regulates the degree of pectin methylesterification in *Arabidopsis* seed mucilage. Plant Cell **25:** 944–959

Voiniciuc C, Schmidt MHW, Berger A, Yang B, Ebert B, Scheller HV, North HM, Usadel B, Günl M (2015a) MUCILAGE-RELATED10 produces galactoglucomannan that maintains pectin and cellulose architecture in Arabidopsis seed mucilage. Plant Physiol **169:** 403–420

Voiniciuc C, Yang B, Schmidt MH, Günl M, Usadel B (2015b) Starting to gel: how Arabidopsis seed coat epidermal cells produce specialized secondary cell walls. Int J Mol Sci **16:** 3452–3473

Walker M, Tehseen M, Doblin MS, Pettolino FA, Wilson SM, Bacic A, Golz JF (2011) The transcriptional regulator LEUNIG_HOMOLOG regulates mucilage release from the Arabidopsis testa. Plant Physiol **156:** 46–60

Warde-Farley D, Donaldson SL, Comes O, Zuberi K, Badrawi R, Chao P, Franz M, Grouios C, Kazi F, Lopes CT, et al (2010) The GeneMANIA prediction server: biological network integration for gene prioritization and predicting gene function. Nucleic Acids Res **38:** W214–W220

Weigel D, Glazebrook J (2006) In planta transformation of Arabidopsis. Cold Spring Harb Protoc **2006:** 107–120

Western TL (2011) The sticky tale of seed coat mucilages: production, genetics, and role in seed germination and dispersal. Seed Sci Res **22:** 1–25

Winter D, Vinegar B, Nahal H, Ammar R, Wilson GV, Provart NJ (2007) An Electronic Fluorescent Pictograph browser for exploring and analyzing large-scale biological data sets. PLoS One **2:** e718

Woody ST, Austin-Phillips S, Amasino RM, Krysan PJ (2007) The WiscDsLox T-DNA collection: an Arabidopsis community resource generated by using an improved high-throughput T-DNA sequencing pipeline. J Plant Res **120:** 157–165

Wu AM, Hörnblad E, Voxeur A, Gerber L, Rihouey C, Lerouge P, Marchant A (2010) Analysis of the Arabidopsis *IRX9/IRX9-L* and *IRX14/IRX14-L* pairs of glycosyltransferase genes reveals critical contributions to biosynthesis of the hemicellulose glucuronoxylan. Plant Physiol **153:** 542–554

Young RE, McFarlane HE, Hahn MG, Western TL, Haughn GW, Samuels AL (2008) Analysis of the Golgi apparatus in *Arabidopsis* seed coat cells during polarized secretion of pectin-rich mucilage. Plant Cell **20:** 1623–1638

Yu L, Shi D, Li J, Kong Y, Yu Y, Chai G, Hu R, Wang J, Hahn MG, Zhou G (2014) CSLA2, a glucomannan synthase, is involved in maintaining adherent mucilage structure in Arabidopsis seed. Plant Physiol **164:** 1842–1856

Zabotina OA, Avci U, Cavalier D, Pattathil S, Chou YH, Eberhard S, Danhof L, Keegstra K, Hahn MG (2012) Mutations in multiple XXT genes of Arabidopsis reveal the complexity of xyloglucan biosynthesis. Plant Physiol **159:** 1367–1384